



Experimental modeling and optimization of surface quality and thrust forces in drilling of high-strength Al 7075 alloy: CRITIC and meta-heuristic algorithms

G. C. Manjunath Patel¹ · Jagadish²

Received: 20 April 2020 / Accepted: 5 March 2021 / Published online: 9 April 2021
© The Brazilian Society of Mechanical Sciences and Engineering 2021

Abstract

Al 7075 is a renowned high-strength engineering material used in automotive and aerospace applications, wherein many functional cylindrical parts are subjected to internal or external loads. Engineered parts with form errors (cylindricity CE and circularity error Ce) result in undesirable vibration and high deformation in rotating parts. In addition, reduced surface roughness (SR) and thrust forces (TF) are essential to limit the secondary process (namely, polishing) and power consumption. Experiments are performed based on central composite design considering drilling parameters (point angle, cutting speed, and feed rate) as inputs and output performances as CE, Ce, TF, and SR. It is noted that, except feed rate for Ce, all other parameters are found significant toward the output performance. Also, prediction accuracy with ten random experimental cases resulted with the percent error of 8.4% for SR, 5.41% for TF, 10.64% for Ce, and 10.35% for CE, respectively. Continuous ribbon-like chips at higher cutting speed, loose fragmented chips at higher feed rate, and increased arc length and radius at higher point angle were observed from the chip morphology analysis. Criteria importance through inter-criteria correlation (CRITIC) method applied to determine the weight fractions for Ce, CE, TF, and SR was found equal to 0.2802, 0.1991, 0.3293, and 0.1914, respectively. Four algorithms (genetic algorithm GA, particle swarm optimization PSO, teaching learning-based optimization TLBO, and JAYA algorithm) were applied to determine the optimal drilling conditions. JAYA algorithm determined optimized drilling conditions ensure predicted output values found close to experimental values with an acceptable percent error of 10.8% for Ce, 8.9% for CE, 6.73% for SR, and 3.51% for TF, respectively.

Keywords Drilling process · Form accuracy · Thrust force · Surface roughness · JAYA · TLBO · PSO and GA

1 Introduction

Aluminum alloys are known for its lightweight with high-strength to weight ratio characteristics, which are used as key engineering materials in automotive and aerospace

applications [1]. The metal cutting processes are applied directly or indirectly in many of the said industrial parts. Drilling (hole making) process alone accounts to 40% of total metal cutting processes, widely used for fastening various parts of industrial applications [2]. Drilling process is one among the most time-consuming process utilizing 36% of all machine hours, compared to 25% for turning, 26% for milling, and others [3]. Therefore, developing an appropriate high-performance drilling system (i.e., control of drilling factors) could significantly reduce the cost, hole quality, and form accuracy of the parts [1–3].

Economics and hole quality of parts are related to drilling operating variables, properties of tool-work piece materials, and so on. Previous findings showed that burr height and surface roughness alter the mechanical properties of drilled Al-alloy (Köklü et al. [4]). Burrs in Al-alloys occur naturally due to their higher ductility and rough surface on the drilled hole (Mohamed et al. [5]). This is attributed to the

Technical Editor: Izabel Fernanda Machado.

✉ Jagadish
jagadish.mech@nitrr.ac.in

G. C. Manjunath Patel
manju09mpm05@gmail.com

¹ Department of Mechanical Engineering, PES Institute of Technology and Management, (Affiliated to Visvesvaraya Technological University, Belagavi) Shivamogga, Shivamogga 577204, India

² Department of Mechanical Engineering, National Institute of Technology, Raipur 492010, India

increased combination of cutting variables (speed and feed) and drill size. Engine blocks, plastic injection molds and dies, aircraft body typically have different hole diameter, depths, and surface finish (Abidin et al. [6], Rivero et al. [7]). Few experimental investigations were carried out with different tool diameters varied in the ranges between 8 and 20 mm, typically used for fastening, and riveting the industrial parts [8–11]. The effect of drilling variables, namely drilling depth, spindle speed, and feed rate on drill bit temperature, was experimentally investigated by Bagci et al. [12]. Point angle of the drill tool showed direct effect on surface roughness of drilled hole (Nouari et al. [13]), and the recommended point angle for aluminum silicon alloys could vary in the ranges between 115° and 140° (Davim [14]). Note that, the point angle used for drilling of AA 6351-B₄C composite and carbon fiber-reinforced composites was varied in the ranges of 70°–118° [8, 15]. Low feed rate and point angle resulted in better-quality drilled holes in the composites [15]. The cutting temperature increases with the increased values of speed and feed rate (Ueda et al. [16]). The effect of point angle was not considered in their research effort. The resulted higher temperature (heat generation) effects on the surface quality, form accuracy and chip morphology (Matsumura et al. [17]). The numerical simulation based on finite volume method was used to estimate the temperature distribution. The developed model does not consider the effect of cutting speed and feed rate, and assumed the chip flow angle on rake face. Such assumptions are difficult to meet in actual practical experiments. Drilling aluminum alloy at higher cutting speeds affects the quality of hole size and forms the built-up edge on twist

drills, which increases the cutting forces (Davoudinejad et al. [18]). Although feed rate and point angle had major effect on hole quality, their effect was neglected in their research findings. The cutting force (i.e., thrust and torque) reduces significantly with increase in cutting speed (Rahim et al. [11]). The material hardness reduces with an increase in cutting temperature as a result of higher cutting speed. Increased feed rate significantly increases the thrust force and torque during drilling process (Rahim et al. [19]). Feed rate contributes more on overcut in drilled holes (Prasanna et al. [20]). In addition to influence of point angle, the effect of cutting speed (Rahim et al. [19]) and feed rate [(Rahim et al. [11]) was neglected in their research analysis. Higher overcut alters the circularity of the drilled hole that results in poor surface finish and improper fits. The cutting forces showed strong dependent relationship with chip thickness and are explained better with the feed rate (Liao et al. [21]). Drilling aluminum alloys generates large amount of chips, and studies showed that the chip dimensions (size and length) vary with drilling variables and tool geometry (in particular point angle) (Batzer et al. [22]). It was confirmed from the above literature review that the cutting variables strongly affect the cutting temperature, thrust forces, surface roughness, chip morphology, and dimensions of the hole quality.

Al 7XXX series (Al–Zn–Mg–Cu) alloys possess highest strength among all aluminum series alloys. Thereby, those alloys are widely accepted in aircraft sectors due to their excellent mechanical properties and resistance to corrosion and fatigue (Knight et al. [23]). Drilling of high-strength aluminum alloy (Al 7075) with different cutting parameters, drill tool materials, and diameters are presented in Table 1. Significant

Table 1 Summary of different investigations of drilling Al7075 alloy

Alloy	Drill diameter & Material	Cutting variables	Responses	Reference
Al 7075	7 mm Coated (Mo, Ti, and Co) HSS	FR (continuous or intermittent): 50 mm/min CS: 25 m/min: TM: Mo-HSS, Ti-HSS, Co-HSS	Thrust forces Surface roughness Torque	[23]
Al 7075-T651	10 mm TiN/TiAlN-coated carbide drills	SS: 1910, 2547, 3184 rpm FR: 0.1, 0.15, 0.2 mm/rev DD: 20, 30, 40 mm	Temperature	[12]
Al 7075	14 mm Coated & uncoated carbide drills	TM: Coated carbide, uncoated carbide FR: 0.1, 0.2, 0.3 mm/rev CS: 170, 200, 230 m/min	Temperature	[25]
Al 7075	5 mm HSS drills	FR: 0.1, 0.2, 0.3 mm/rev CS: 4, 12, 20 m/min PA: 90, 118, 135°	Burr height Surface roughness	[26]
Al 7075	5 mm TiN/TiAlN-coated & HSS drills	SS: 910, 1420, 2000 rpm FR: 0.06, 0.08, 0.1 mm/rev DP: 4, 5, 6 mm	Surface roughness Roundness Enlargement	[27]
Al 7075-T6	8 mm Wc–Co-coated drills	CS: 60, 90, 120, 150 m/min FR: 0.05, 0.1, 0.2 mm/rev	Thrust force Torque	[28]

Mo molybdenum, Ti titanium, Co cobalt, HSS high-speed steel, FR feed rate, CS cutting speed, TM tool materials, DP depth packing, DD drilling depth, SS spindle speed, PA point angle

investigations are carried out with different drill material (coat and un-coat), cutting variables, tool vibration, environment (dry and coolant), and drill geometry [12, 24–28]. The said aforementioned studies focused with an aim to minimize the frictional temperature, thrust force, torque, surface roughness, burr height, and roundness error. Note that, experiments are conducted by varying one factor at a time approach. This approach can only estimate the individual factor effect, and the recommended optimal drilling conditions with this approach results in local solution. The estimation of effects of individual and interaction among the factors is indeed essential to provide the complete insight of detailed understanding of a process and derive global solutions. Not much research efforts are being made to detail the insight of both individual and combined effect of factors on the responses.

Design of experiment (DOE) based on response surface methodology (RSM) enables to conduct minimum experiments and collect output data, analyzes factor effects, and derives regression equations useful for predictions. Taguchi method was used to estimate the factor (coated and uncoated tools, cutting speed, and feed rate) effects on cutting temperature of Al 7075 material [25] and surface roughness of AISI 304 steel [29]. Interaction factor effects and impact of point angle were not estimated in their analysis. Taguchi method employed to perform experiments with the influencing parameters (cutting speed, feed rate, and point angle) and analyzed their effects on surface roughness and burr height of holes drilled on aluminum material [26]. The factor effects on dimension errors or hole quality (i.e., cylindricity errors and circularity errors) and thrust force were neglected in their research efforts. Furthermore, authors failed to test the prediction accuracy with random experimental cases. The influence of cutting speed, feed rate, and cutting environment on surface roughness of AISI 1045 parts was studied by applying RSM method [30]. Note that, GA determined optimal drilling conditions resulted with lower surface roughness values. The above literature review confirmed that RSM is an effective tool to provide detailed insight of a process and derive response equations which are useful for performing prediction. Furthermore, no work reported in the literature on multi-objective optimization for better-quality drilled hole.

To remain competitive in world market, maintaining and improving better-quality drilled holes are of industrial relevance. In drilling process, applying optimization techniques with meta-heuristic algorithms helped to solve many problems related to machining time [6, 31], tool path movement [32], cost [6], and surface roughness [30]. GA optimizes the drilling parameters for better performances (surface roughness, delamination factor, and thrust force) in carbon fiber-reinforced epoxy composite [33]. PSO reduces the burr size that minimizes the cost and time by determining optimal condition in drilling AISI 316L stainless steel [34]. The

performances of TLBO and JAYA algorithm were evaluated in determining optimal conditions for plasma arc machining process [35]. Multiple objective optimization requires determining weight fraction for individual objective function. Applying CRITIC method determines the weight fraction for multiple objective functions [36, 37]. Till date, there is no universal standard rule defined yet in selection of optimization techniques for particular application. Therefore, significant scope still exists to apply various optimization techniques and compare those results (output performances) that derive best optimal conditions for a drilling process.

Although a lot of research work published on drilling process and its mechanism, only a few applications explained the effect of variables and developed input–output relationships of drilling process. Many research efforts left out either the most important machining quality characteristics (hole quality: cylindricity and circularity) or they could not apply effective modeling tools that analyze and optimize the drilling process. Furthermore, not much research efforts are made in the literature with a major focus on the following,

- CCD-based nonlinear modeling of a drilling process to know the full quadratic (main, square, and interaction) factor effects on the drilling quality characteristics (SR, TF, CE, and Ce) with drilling variables (i.e., cutting speed, feed rate, and point angle) is yet to be explored.
- Development of experimental-based prediction model (empirical response equations) for a drilling process is not done yet.
- To confirm models for practical utility in industries by conducting the prediction tests.
- To know the relationship among the drilling quality characteristics.
- To know the formation of chip morphology with drilling parameters.
- To determine the weight fractions for each quality characteristics.
- To perform multi-objective (SR, Ce, CE, and TF) optimization using meta-heuristic algorithms for a drilling process.

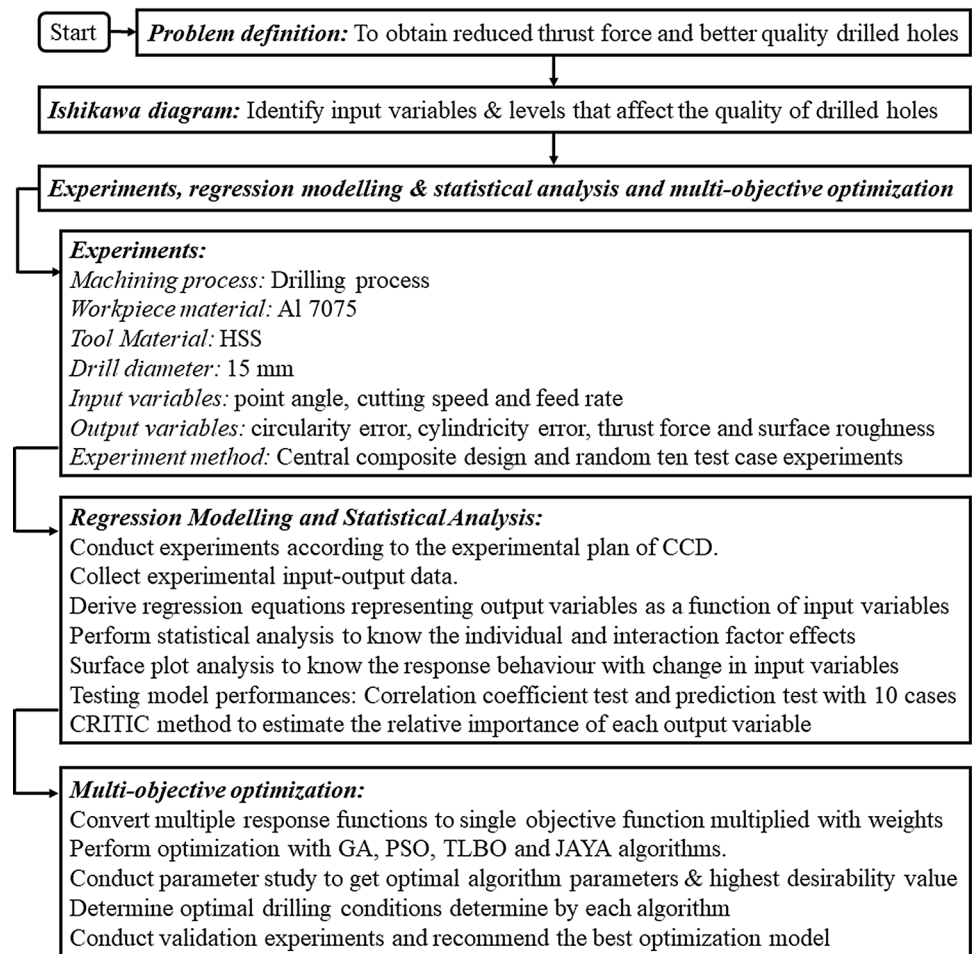
The methodology employed for experimental modeling, analysis, and optimization of drilling process for better drilled hole quality with reduced thrust force is presented in Fig. 1

2 Materials and methods

2.1 Materials and experimental setup

Drilling experiments are conducted using BATLIBOI radial drilling machine. The machine is capable to drill hole up to

Fig. 1 Framework illustrating the methodology employed for experimental modeling and optimization



60 mm. Drill tool dynamometer measures the thrust force during the drilling experiments. The work material used is Al 7075 (Al-88%, Zn-6%, Mg-2.8%, Cu-1.6%, Si-0.4%, Fe-0.4%, Mn-0.3%, Cr-0.2%, Ti-0.2%, others-0.1%) and is supported with wooden board and is clamped tightly with the fixture. The wooden support board is to protect the dynamometer and to eject the chips from the exit side of the drill (refer Fig. 2). The thrust force is directly recorded during each experimental trial. HSS twist drills (15 mm diameter) with three different point angles were used for experimentation and analysis (refer Fig. 2).

Prior to experiments, the Al 7075 plates were ground and cleaned to remove the surface defects (present if any). Experiments are performed under dry cutting environment to perform blind holes of depth 20 mm. To attain center drill initial marking on the work sample is done with the help of dot punch. Figure 3 shows the probable factors that influence the quality (productivity, economy, form accuracy, surface finish, energy, and so on) of the drilled hole, which are clearly observed from detailed literature review [8–11, 15, 24, 26–28, 38, 39].

2.2 Selection of factors and levels

In the present work, control factors (i.e., cutting speed, feed rate, and point angle) and their levels for experiments are set through experts' judgment and conducting pilot experiments. During pilot experiments, individual factors such as cutting speed, feed rate, and point angle showed dominant effect on the output quality characteristics. Following experimental observations are made while deciding factor levels: Higher feed rate and cutting speed resulted in increased burr height and in turn affect the quality (circularity, cylindricity, and surface roughness) of drilled holes. However, drilled hole quality was improved with the mid-values of point angle. Reduced values of thrust force and surface roughness were observed with low values of cutting speed and feed rate. From the above experimental observations and consulting literature [16, 19, 20, 24, 25, 39] the levels for each factor were set (refer Table 2). Experiments were performed at three levels of control factors which are critical to the drilling quality characteristics (SR, TF, Ce, and CE). Figure 4 shows the details of fixed and control input variables

Fig. 2 Experimental setup of drilling process

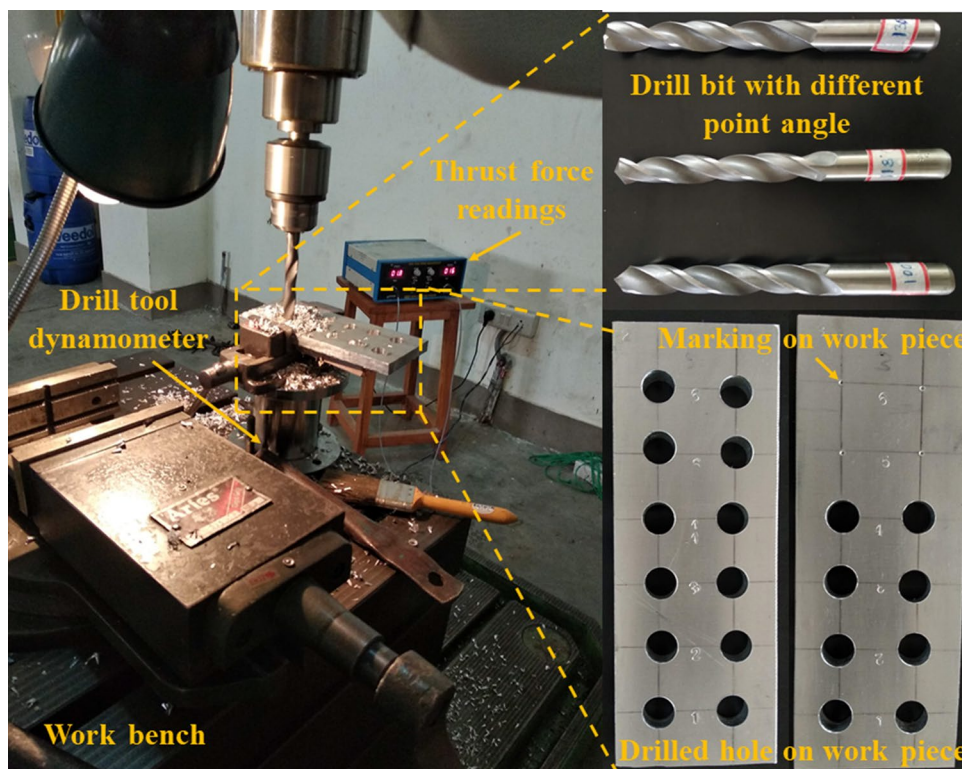


Fig. 3 Fishbone diagram for drilling process

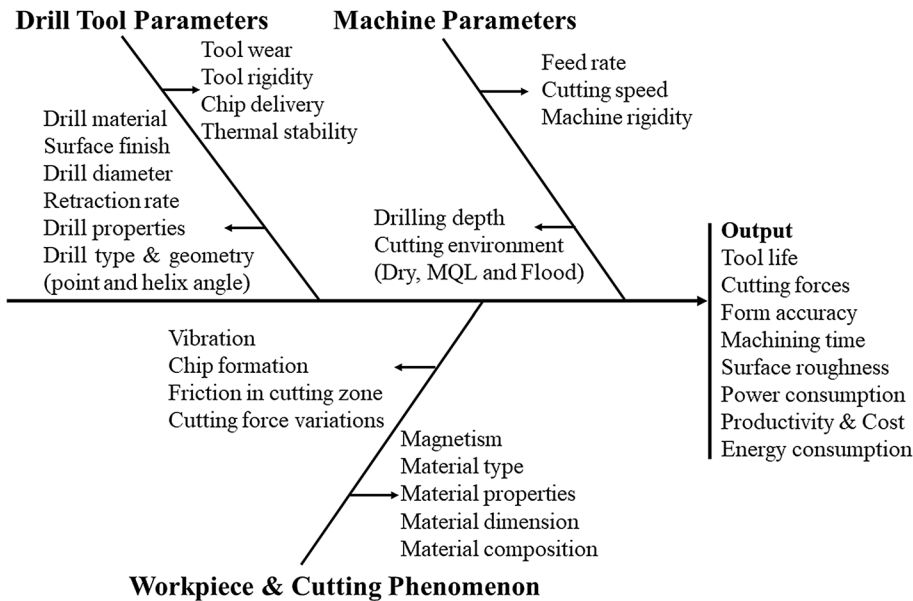
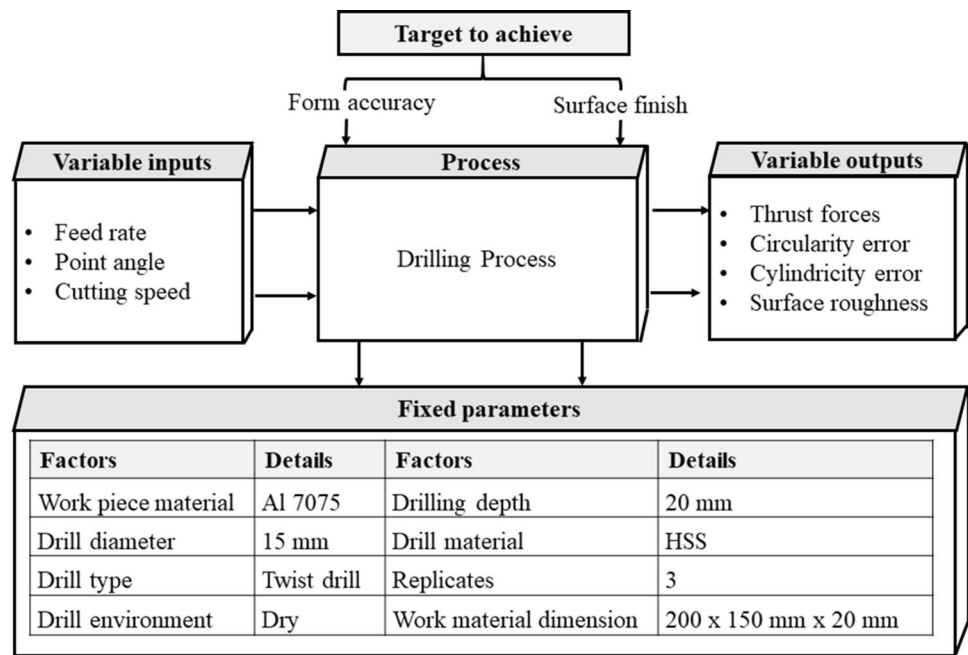


Table 2 Control factors and levels of drilling process

Factors	Notation	Levels (low, middle, and high)
Cutting speed (CS), in m/min	A	8, 14, and 20
Feed rate (FR), in mm/rev	B	0.13, 0.18 and 0.25
Point angle (PA), in deg (^o)	C	100, 118, 135

influencing outputs of a drilling process. To minimize the twisting effect of drill tool (present if any), 30 mm of constant distance has been maintained between the tool tip and workpiece top surface.

Fig. 4 Fixed and controllable input factors influencing outputs for a drilling process



2.3 Measurement of drilling quality characteristics and data collection

Drilling experiments are conducted according to the matrices of response surface design (three-level central composite design, CCD). The experimental matrices composed of three factors and levels are presented in Table 3. Each experiment is repeated thrice, and the average values of thrust forces, surface roughness, cylindricity, and circularity errors are taken for analysis (refer Table 3). The drilled

hole surface roughness was measured on a portable surface roughness tester, i.e., Mitutoyo SJ-301. JIS 2001 standard was employed for performing surface roughness measurements. The cutoff and traversing length values are 0.8 and 2.4 mm, respectively. Total of nine surface roughness values are measured on three replicates (on each replicate, three measurements are taken at the middle of hole wall and parallel to hole axis) of each experimental trial. The average values of nine surface roughness readings corresponding to each drilling conditions are presented in Table 3.

Table 3 CCD experimental data of drilling process

Exp. no	Process variables			Responses			
	A, m/min	B, mm/rev	C, °	SR, μm	TF, KN	Ce, mm	CE, mm
1	20	0.13	100	0.86	1.38	0.093	0.022
2	08	0.13	100	0.91	1.31	0.418	0.045
3	20	0.25	100	1.24	1.90	0.060	0.009
4	08	0.25	100	1.85	2.00	0.392	0.044
5	14	0.18	100	1.05	1.53	0.157	0.010
6	14	0.25	118	1.70	2.44	0.447	0.074
7	20	0.18	118	1.05	1.79	0.089	0.009
8	14	0.18	118	1.48	1.96	0.204	0.028
9	14	0.18	118	1.64	1.91	0.214	0.029
10	08	0.18	118	1.88	1.96	0.388	0.033
11	14	0.13	118	1.26	1.60	0.443	0.055
12	20	0.13	135	1.61	1.48	0.180	0.011
13	14	0.18	135	1.76	2.06	0.223	0.020
14	08	0.13	135	1.85	1.66	0.430	0.052
15	08	0.25	135	3.10	2.45	0.521	0.091
16	20	0.25	135	1.12	2.15	0.190	0.029

Thrust force was measured on three replicates of each experimental trial with the help of drill tool dynamometer. The linearity and accuracy of drill tool dynamometer are found equal to $\pm 1\%$ of full scale. The drill tool dynamometer setup comprises of cable connector, sensors, amplifier, and digital indicator that display the thrust force. The average values of three thrust force measurements were recorded corresponding to each experimental run that is presented in Table 3. The form accuracy (circularity and cylindricity error) of the drilled hole was measured with the help of COMET L3D Tripod a column-type 3D scanner. The value corresponding to largest undercut (+ deviation) added to the absolute value of largest over cut (- deviation) tested on cylindrical sample is termed as cylindricity error. The radial distance between the 2 concentric circles separated by minimum distance and containing all points on the given profile. The scanner transforms the physical component (drilled holes) in to digital form which contains the geometrical feature information of the machined part. Few sample measurement values of drilled holes are shown in Fig. 5. This information is used to determine the circularity and cylindricity errors. Information corresponds to the measurement of circularity, and cylindricity errors are discussed in the literature [40]. The average values of three measurements

of circularity error and cylindricity error are presented in Table 3.

2.4 Criteria importance through inter-criteria correlation (CRITIC) method

Diakoulaki proposed the CRITIC method to determine the weight fractions for each objective function, which are essential to solve multiple objective optimization problems. Multiple objective functions generate many potential solutions, which are analogous to weights assigned to the individual response. Assigning maximum weight fraction to one output could result in compromising solution to the other response. CRITIC method derives weight fractions by combining the contrast intensity and conflict (objective function comprises of both maximization and minimization type) nature involved in decision-making problem. The steps involved in determining the objective weights by applying CRITIC method are as follows [41, 42],

Step 1 Establish the decision matrix (D) comprising of set of m feasible alternatives of experimental design and n evaluation criteria (i.e., quality characteristics). The decision matrix $D = [d_{ij}]$ is expressed with the output value of i th alternative associated with j th criteria.

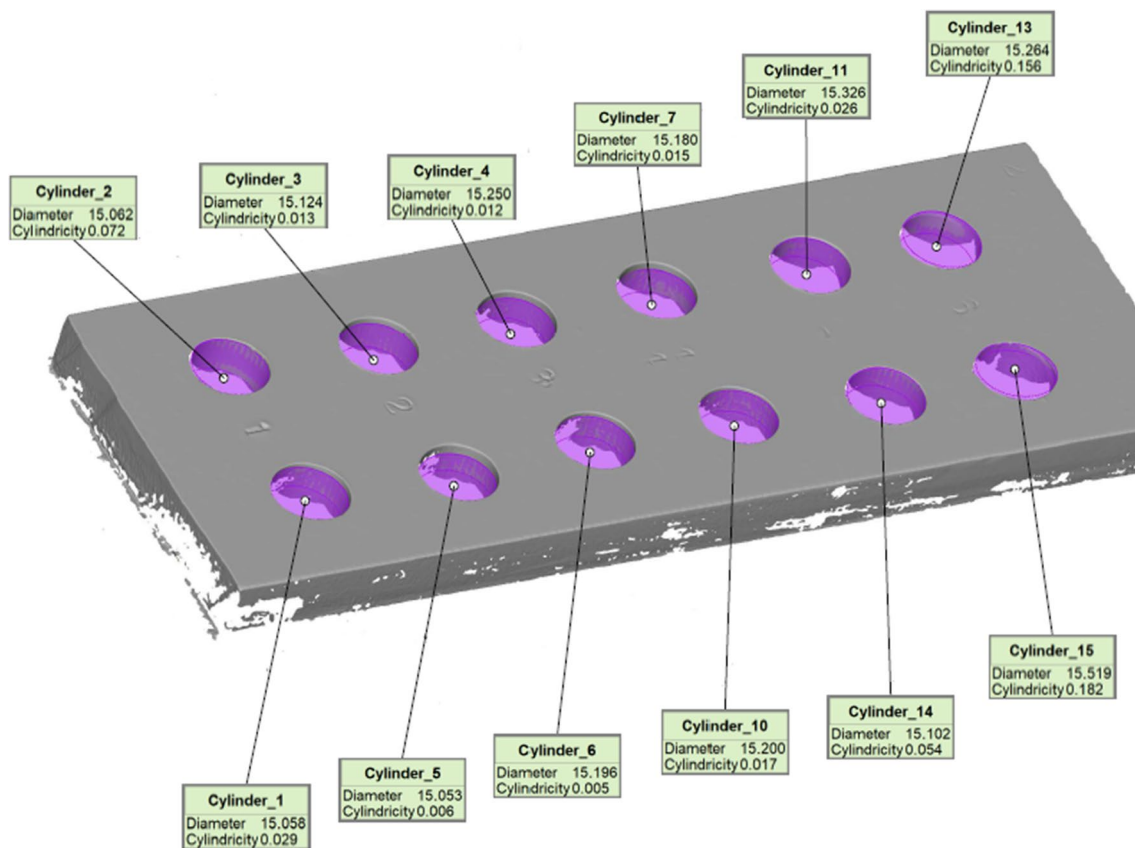


Fig. 5 Sample measurements of circularity and cylindricity errors of drilled holes

$$D = [d_{ij}]_{m \times n} = \begin{bmatrix} d_{11} & d_{12} & \dots & d_{1m} \\ d_{21} & d_{22} & \dots & d_{2m} \\ \dots & \dots & \dots & \dots \\ d_{n1} & d_{n2} & \dots & d_{nm} \end{bmatrix} \quad (i = 1, 2, \dots, m; \text{ and } j = 1, 2, \dots, n) \tag{1}$$

Step 2 The defined decision matrix is normalized (to avoid numerical fluctuations of output values of different quality characteristics) in the ranges between zero and one using Eq. 2.

$$\bar{d}_{ij} = \frac{d_{ij} - d_j^{\text{worst}}}{d_j^{\text{best}} - d_j^{\text{worst}}} \tag{2}$$

where the term \bar{d}_{ij} refers to the normalized output value of *i*th alternative for *j*th criterion and the term d_j^{worst} , d_j^{best} depicts the worst and best value of output of *j*th criterion.

Step 3 The criteria contrast intensity is determined based on standard deviation of normalized criterion values by columns (d_j). The standard deviation of each criterion is estimated using Eq. 3.

$$\sigma_j = \sqrt{\frac{\sum_{i=1}^m (\bar{d}_{ij} - \bar{d}_j)^2}{m}} \tag{3}$$

where term *m* denotes the number of experiments and \bar{d}_j is the average output values of *j*th criterion.

Step 4 Establish the symmetric matrix (*m* × *m*) with the term r_{jk} (i.e., linear correlation coefficient between the criteria's (refer Eq. 4)).

$$r_{jk} = \frac{\sum_{i=1}^m (\bar{d}_{ij} - \bar{d}_j)(\bar{d}_{ik} - \bar{d}_k)}{\sqrt{\sum_{i=1}^m (\bar{d}_{ij} - \bar{d}_j)^2 \sum_{i=1}^m (\bar{d}_{ik} - \bar{d}_k)^2}} \tag{4}$$

Step 5 The product of Eq. 3 and 4 determines the criterion information (C_j).

$$C_j = \sigma_j \sum_{k=1}^m 1 - r_{jk} \tag{5}$$

Step 6 The weights of each individual output are determined by applying normalizing technique with the help criterion information as shown in Eq. 6.

$$W_j = \frac{C_j}{\sum_{j=1}^n C_j} \tag{6}$$

2.5 Multi-objective optimization

The multi-objective optimization for drilling process is to determine the output values with less quality variation in

the parts within the acceptable range. Surface plot analysis and significance test results showed that the quality characteristics (SR, TF, Ce, and CE) vary complex (both linear and nonlinear) with the cutting parameters of drilling process. Realizing the complexity and dynamics involved in drilling process, the development of advanced optimization tools (metaheuristic algorithms) is indeed essential to determine the global solution for each quality characteristics. GA and PSO are the popular meta-heuristic search algorithms applied in the past to solve machining process optimization problems [26, 43]. Ant lion optimization (ALO), Grey wolf optimizer (GWO), TLBO, cat swarm optimization, cuckoo search (CS), JAYA algorithm, etc., were applied to solve many engineering problems in the last decade [44–52]. TLBO and JAYA algorithm outperformed other algorithms, when tested for different case studies of mechanical engineering problems [53, 54]. The performances are evaluated based on the number of function evaluation, solution accuracy, and computational efforts and time. In the present work, four algorithms were applied to optimize the multiple responses for the set of input variables, and their performances are evaluated mainly with desirability function approach (DFA).

2.5.1 Desirability function approach

DFA evaluates how best the set of input factors satisfy the pre-defined goal (maximization or minimization) for the responses. The present work requires optimization of composite responses (overall desirability, D_o) for the input variable setting. The overall desirability value varies between the range of zero and one. The D_o value close to one could be the ideal value for any process optimization. The overall desirability value is treated as fitness function for the optimization problem. The computation of overall desirability value considering all responses is done using Eq. 7.

$$D_o = \sqrt[4]{(d_{Ce}^{W_1} \times d_{CE}^{W_2} \times d_{SR}^{W_3} \times d_{TF}^{W_4})} \tag{7}$$

where the terms, W_1 , W_2 , W_3 and W_4 , are the weights corresponding to Ce, CE, SR, and TF. The weights of each response are determined with the help of CRITIC method. In the present work, Ce, CE, SR, and TF need to be optimized to get a minimum value of each response and their desirability value computation is done by applying Eq. 8.

$$d_{Ce} = \frac{Ce_{\max} - Ce}{Ce_{\max} - Ce_{\min}}, \quad d_{CE} = \frac{CE_{\max} - CE}{CE_{\max} - CE_{\min}},$$

$$d_{SR} = \frac{SR_{\max} - SR}{SR_{\max} - SR_{\min}}, \quad d_{TF} = \frac{TF_{\max} - TF}{TF_{\max} - TF_{\min}} \tag{8}$$

where the term Ce_{\max} , CE_{\max} , SR_{\max} , and TF_{\max} are the maximum values and Ce_{\min} , CE_{\min} , SR_{\min} , and TF_{\min} represent the

minimum values of Ce, CE, SR, and TF, respectively. While the terms d_{Ce} , d_{CE} , d_{SR} , and d_{TF} are the desirability index corresponding to Ce, CE, SR, and TF, respectively.

2.5.2 Genetic algorithm

Charles Darwin theory of survival of fittest is employed in genetic algorithm to determine the potential solutions for many engineering problems [55]. GA has many advantages over traditional algorithms (i.e., programming methods: goal, sequential, dynamic, nonlinear, geometrical, etc.) to solve problems involving different variable, objective, and constraints [54, 56]. Although GA conducts heuristic search, their performances are dependent on the population size, diversity of individual solutions in search space, crossover, and mutation. Parameter study is carried out to tune the genetic parameters that could locate the global desirability value for the optimization problem.

2.5.3 Particle swarm optimization

PSO mimics the foraging behavior of bird flock to solve many engineering problems (Karaboga et al. [56]). To limit the difficulties in determining the appropriate parameters (crossover, mutation, selection method, etc.) of genetic algorithm and to avoid premature convergence present if any, PSO is developed. PSO conducts faster search, as it requires few tuning parameters (inertia weight, acceleration coefficients) with relatively easy to understand and apply to solve complex optimization problems (Ding et al. [57]). PSO is a popular swarm intelligence algorithm, wherein swarm is a group or community entails many solutions, and each solution is referred as a particle. Each particle flies in a multi-dimension search space with certain position and velocity. The particle adjusts their flight path according to neighboring and their own flying experience while conducting optimal solutions in a multi-dimensional space (Sierra et al. [58]). The PSO parameters (inertia weight, swarm size, and maximum number of iterations) are tuned to determine the global desirability value that could result in optimal conditions for drilling process.

2.5.4 Teaching–learning-based optimization

Rao et al. [51] proposed TLBO algorithm with the idea of teachers influence on learners in a class. TLBO mimics the teaching–learning ability of learners and teachers in a classroom. TLBO algorithm has been developed to limit the disadvantages of tuning of algorithm-specific parameters (GA requires tuning of crossover, mutation rate; PSO requires tuning of inertia weight and acceleration coefficients). There is no universal acceptable value and standards defined yet to determine the algorithm-specific parameters. Those values

are problem specific, and improper tuning of algorithm-specific parameters could result in increased computation time and local solutions [51, 52]. TLBO requires tuning of only common parameters such as population size and iterations. TLBO works with two phases, wherein learning with the help of teacher in teaching phase and by mutual interaction among learners in learning phase. In TLBO, the output results in terms of grades or marks of learners are analogous partly by the impact of teacher. In general, teacher is highly qualified trained professional who educate learners to improve their grades. It is also true that the interaction among learners could also improve their results. In TLBO, group of learners are treated as population and different subjects offered are design variables and learner's outcome is the fitness value of the problem domain. The key task of teacher and learner phases involved in TLBO process is discussed below,

Teacher phase: Teacher will train the learners in a class with a major aim to enhance the average class performance for the subject taught by him/her to their best gained knowledge. The mathematical steps involved in determining the best learner, teaching factor, and difference of existing solution updated in teacher phase are explained earlier in the literature [47, 52]. The updated and accepted solutions after the completion of teacher phase are stored and treated as input to the learner phase.

Learner phase: Learners try to enhance their accumulated knowledge gained from teacher, through randomly interacting with other learners. In this phase, learners may learn new things with the possibility that the other learners possess better knowledge or skills than him or her. The mathematical steps involved in the learner phase are explained in the literature [47, 52]. The accepted and updated solutions of learner phase are treated as input to teacher phase for next iteration. The teacher and learner phases are repeated till the predefined termination criteria are met.

2.5.5 JAYA algorithm

In 2016, Rao proposed one more algorithm-specific parameter less algorithm named as JAYA (Sanskrit word meaning victory) [48]. JAYA algorithm developed with the idea of solution determined for a given problem that moves toward best and avoids the worst solutions [49]. However, TLBO algorithm does not require tuning of algorithm-specific parameters, requires two phase (teacher and learner phase) evaluation to determine the solutions that result in increased computation time. JAYA algorithm thus developed to work with only one phase that offers reduced computation time and efforts to implement. The mathematical steps involved in working of JAYA algorithm are explained in the literature [48, 49, 53, 54].

3 Results and discussion

This section describes the analysis of results of the models developed for the collected experimental input–output data. The empirical equations derived for predictions are tested for ten random experiments. The chip formations under different cutting conditions are also discussed. The weight fraction of each responses is determined by applying CRITIC method. The optimal cutting condition for the multiple outputs is determined using advanced algorithms.

3.1 Model development and analysis

Experimental input–output data collected as per the design matrices were used to develop the models and perform analysis. The response-wise analysis and their corresponding results obtained from the drilling process are discussed below,

3.1.1 Surface roughness

The second-order response surface model for surface roughness is expressed mathematically to establish relationship with cutting variables as shown in Eq. 9.

$$SR = -7.23 + 0.271A + 21.2B + 0.0627C + 0.00124A^2 + 5.1B^2 - 0.000017C^2 - 0.790AB - 0.001862 AC - 0.0666BC \tag{9}$$

The full quadratic terms (linear: A, B, C ; square: A^2, B^2, C^2 ; interaction: $A \times B, A \times C, B \times C$) tested at 95% confidence level are presented with ANOVA Table 4. P values of terms ($A, B, C, A \times B$, and $A \times C$) were found less than 0.05 and hence found to be significant for SR (refer Table 5). Cutting speed found to have maximum effect followed by point angle and feed rate. The P values of all square terms of drilling parameters (CS, FR, and PA) are greater than 0.05, which signifies that the surface roughness relationship with drilling parameters is found to be linear. The results of statistical tests (significance of factors) are found to have good relationship with the surface plots (refer Fig. 6a–c). Although all linear or main effect factors are significant, the interaction term $B \times C$ (FR and PA) is found insignificant. Lack of fit exists for the surface roughness model, and removing noncontributory terms makes the model statistically significant (refer Table 4). Insignificant terms (A^2, B^2, C^2, BC) can be removed from the model by backward elimination method. In Eq. 7, removing insignificant terms reduces prediction accuracy as a result of imprecise input–output relationship. This occurs because the estimated F-statistics results in higher value than Table F value. Therefore, excluding insignificant terms from the regression equations is not to be recommended. The P values

Table 4 Results of ANOVA test for TF and surface quality (SR, Ce, and CE)

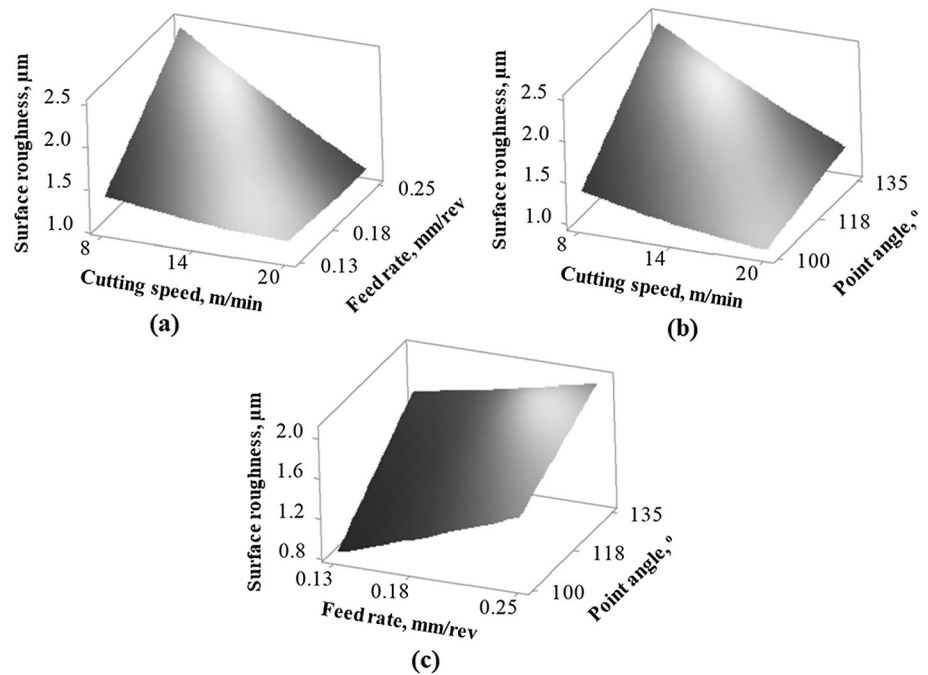
Responses	Circularity error, Ce				Cylindricity error, CE					
	Source	DF	Adj. SS	Adj. MS	F value	P value	Adj. SS	Adj. MS	F value	P value
Model	9	0.335841	0.037316	25.30	0.000	0.008461	0.000940	40.84	0.000	
Linear	3	0.255938	0.085313	57.84	0.000	0.004415	0.001472	63.92	0.000	
Square	3	0.075058	0.025019	16.96	0.002	0.002883	0.000961	41.75	0.000	
2TI	3	0.005029	0.001676	01.14	0.407	0.001047	0.000349	15.15	0.003	
Error	6	0.008850	0.001475			0.000138	0.000023			
Lack of fit	5	0.008800	0.001760	35.20	0.127	0.000138	0.000028	55.05	0.102	
Pure error	1	0.000050	0.000050			0.000001	0.000001			
Total	15	0.344691				0.008599				
Responses	Surface roughness, SR				Thrust force, TF					
Source	DF	Adj. SS	Adj. MS	F value	P value	Adj. SS	Adj. MS	F value	P Value	
Model	9	4.27757	0.47529	12.10	0.003	1.70900	0.18989	28.50	0.000	
Linear	3	3.30252	1.10084	28.02	0.001	1.56342	0.52114	78.23	0.000	
Square	3	0.01032	0.00344	00.09	0.964	0.12686	0.04229	06.35	0.027	
2TI	3	0.99460	0.33153	08.44	0.014	0.04160	0.01387	02.08	0.204	
Error	6	0.23573	0.03929			0.03997	0.00666			
Lack of fit	5	0.22293	0.04459	03.48	0.385	0.03872	0.00774	06.20	0.296	
Pure error	1	0.01280	0.01280			0.00125	0.00125			
Total	15	4.51330				1.74898				

DF: degrees of freedom; Adj. SS: adjusted sum squared error; Adj. MS: adjusted mean squared error; 2TI: 2 term interaction

Table 5 Significance test results of different responses

Responses	Correlation coefficient		Variables	
	All terms (significant & insignificant)	Excluding insignificant terms	Significant	Insignificant
Circularity error, Ce	0.9743	0.9358	A, C, B ² , C ²	B, A ² , AB, AC, BC
Cylindricity error, CE	0.9839	0.9598	A, B, C, A ² , B ² , C ² , AB, AC, BC	NIL
Surface roughness, SR	0.9478	0.8694	A, B, C, AB, AC	A ² , B ² , C ² , BC
Thrust force, TF	0.9771	0.9429	A, B, C, C ²	A ² , B ² , AB, AC, BC

Fig. 6 3D surface plots for SR with: **a** CS and FR, **b** CS and PA, **c** FR and PA



of composite effect of linear and interaction terms are found less than 0.05, and R^2 value for surface roughness is found to be 0.9478 (close to 1). Therefore, the nonlinear model for the surface roughness is statistically adequate with better fit.

Figure 6a–c shows the 3D plot of surface roughness expressed with the function of cutting parameters (CS: A, FR: B, and PA: C). The desired low surface roughness values are attributed to higher cutting speed (20 m/min) and low values of feed rate (0.13 mm/rev) and point angle (100°). Similar trend results are observed and found good agreement with literature [8]. At low cutting speed, the chips generated during the drilling process will be in the form of segmented or discontinuous. The discontinuous chips affect the surface texture of drilled hole during chips ejection through flutes, in addition to increased vibration. The vibration and chip thickness increase, with the corresponding increase in feed rate that causes poor surface finish. Figure 6b–c shows that the surface roughness increases with the point angle. This occurs due to the clearance to be established between the tool and workpiece interface reduces, which increases the

flank wear on tool surface that causes poor surface on drilled holes.

3.1.2 Thrust force

The thrust force expressed as a mathematical nonlinear function of drilling parameters is shown in Eq. 10.

$$\begin{aligned}
 TF = & -7.43 + 0.1262A + 2.56B + 0.1252C \\
 & - 0.002A^2 + 4.2B^2 - 0.000481C^2 \\
 & - 0.0983AB - 0.000537AC + 0.0262BC \quad (10)
 \end{aligned}$$

Table 5 shows the significant and insignificant terms identified for thrust force. All linear parameters are found significant, with feed rate being the maximum contribution and least by cutting speed toward the response–thrust force. The square term of point angle (C^2) is significant, and the relationship with thrust force is found to be nonlinear in nature (refer Fig. 7b–c). The feed rate and cutting speed of square terms were found insignificant and showed linear relationship with thrust force (refer Fig. 7a–c). The

interaction among the drilling parameters is insignificant toward this response (refer Tables 4 and 5). This signifies the interaction effects among the drilling parameters (CS x FR, CS x PA, FR x PA) are less toward thrust force. The composite effect of all linear and square terms was found to be less than 0.05. Although the composite of all interaction factors is insignificant (P value = 0.204, > 0.05), the developed model produced better fit with an R^2 value found equal to 0.9771. Thereby, the model developed for thrust force is statistically adequate to make better prediction.

Figure 7a–b shows the interaction effect of cutting speed with FR and PA on TF. Cutting speed showed less contribution compared to feed rate and point angle. The resulted thrust force variation with the cutting speed is seen to be of almost flat. Thrust force found to increase initially and decrease toward higher cutting speed. This might be due to the thermal softening of the material as a result of heat generation caused with the increase in cutting speed. Higher cutting speed minimizes the friction coefficient on tool face resulted in low thrust force [2, 8]. Increase in feed rate, increases the cutting area which tends to wear out the chisel edge of drill tool that could resulted in higher thrust force (refer Fig. 7 a-c). In addition, as feed rate increases, the undeformed chip cross-sectional area also increases resulted in greater chip deformation which tends to increase the thrust force [19]. Thrust force increases with the increased values of drill tool point angle (refer Fig. 7b–c). The increased values of point angle tend to increase the feed force while drilling the composite materials [59]. Increase in point angle tends to widen the lip angle of the drill tool and requires larger force for the tool to penetrate the work

piece in an axial direction. The desired minimum thrust force values are observed at the low levels of CS, FR, and PA.

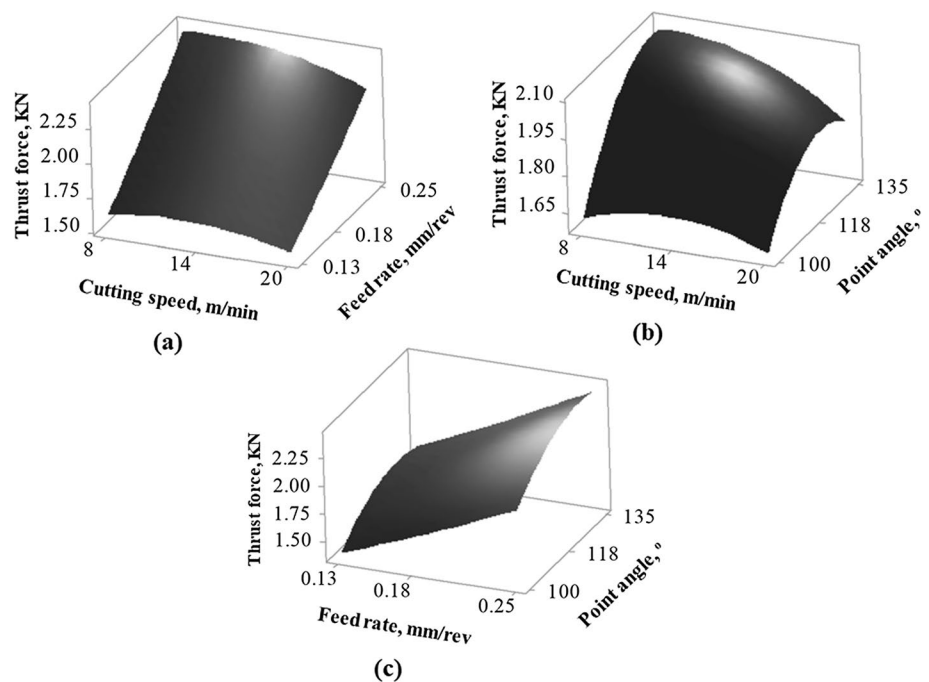
3.1.3 Cylindricity error

The mathematical nonlinear function relating CE with drilling parameters is presented in Eq. 11.

$$\begin{aligned} \text{CE} = & -0.349 + 0.01308A - 4.270B + 0.01157C \\ & - 0.000272A^2 + 9.321B^2 - 0.000051C^2 \\ & - 0.01216AB - 0.000053AC + 0.00852BC \quad (11) \end{aligned}$$

The full quadratic terms of Eq. 11, are tested for parameter significance at 95% confidence level. Table 5 shows the significant and insignificant factors determined for CE. Interesting to note that the P values of all the full quadratic terms (A , B , C , A^2 , B^2 , C^2 , $A \times B$, $A \times C$, and $B \times C$) are significant for this response. The square terms of all the cutting factors (CS, FR, and PA) are significant, which indicate their relationship with cylindricity error is nonlinear. The cutting speed is found to have maximum impact and feed rate being the least effect on cylindricity error. Furthermore, all cutting factor interactions (CS x FR, CS x PA, PA x FR) are found statistically significant toward the cylindricity error. These interaction terms in the response equation are found to make significant effect on cylindricity error. The model developed for cylindricity error resulted in better coefficient of correlation with a value equal to 0.9839. The better fit produced by the model ensures they are statistical adequate for making better prediction.

Fig. 7 3D surface plots for TF with: **a** CS and FR, **b** CS and PA, **c** FR and PA



Cylindricity error variations are with the interaction effect of CS with FR and PA (refer Fig. 8a–c). The desired minimum cylindricity error is observed near the low values of point angle, middle values of feed rate, and at higher cutting speed. The effect of feed rate and cutting speed showed similar trend to get better form accuracy of drilled hole in the published literature [19]. Higher feed rate is practically not recommended due to frictional heating coupled with plowing effect, and conversely high values of cutting speed resulted in better rotational stability that leads to reduced cylindricity error [60]. Increase in cutting speeds produces continuous chips rather than segmented chips at low speed, which alters the surface texture of the drilled hole. Thermal softening of material occurs at higher cutting speed which not only reduces the cutting force, but also creates chatter and vibration in cutting tool that might result in reduced cylindricity error. Increased feed rate allows the cutting tool to penetrate at faster rate toward the workpiece, resulted in increased cutting forces, hole deflection, and vibration that causes higher cylindricity error. Low feed rates coupled with high cutting speed produce good rotational stability, which ensures the drill bit pierce the work material without vibration resulted in lower circularity and cylindricity error [61]. It is well-known fact that with the increase in point angle the lip angle of the drill tool widens that causes increase in thrust force and affects the dimension errors (i.e., cylindricity errors). Better drilled hole quality (dimension error) is observed with reduced point angle while drilling biocomposites [39].

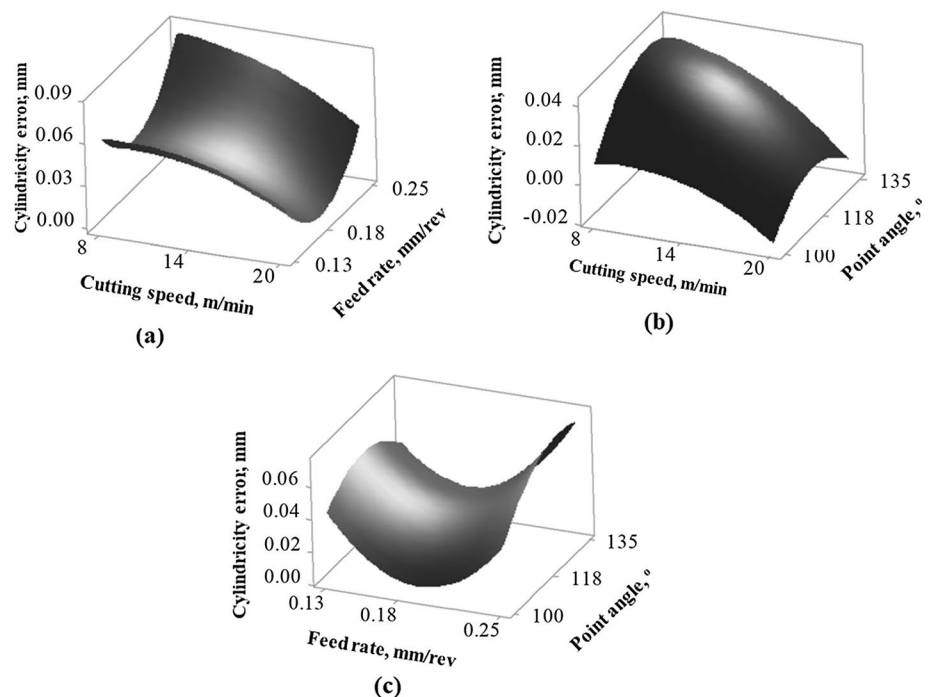
3.1.4 Circularity error

The circularity error is mathematical expressed as a nonlinear function with the drilling variables as shown in Eq. 12.

$$Ce = -1.69 + 0.0013A - 19.66B + 0.0652C - 0.001133A^2 + 47.1B^2 - 0.000288C^2 - 0.0308AB + 0.000091AC + 0.0193BC \quad (12)$$

Full quadratic terms (linear, square, and interaction) are tested for their practical significance at 95% confidence level. Feed rate is found to have insignificant for circularity error, and this occurs due to the low values of generated axial forces during drilling. Axial forces majorly occur at the drill tool center which are influenced by the feed rate. In addition, the square terms of feed rate and point angle were found to significant, which indicates their relationship with the circularity error is nonlinear (refer Table 5). There is no interaction effect among the factors observed as their P values are found to be greater than 0.05 (refer Table 4). The model developed for circularity error in relationship with drilling parameters is found to have good correlation coefficient with a value equal to 0.9743. The model developed and derived empirical relationship to predict the circularity error for known set of drilling parameters around the design points can be effectively utilized for their practical utility in industries. The surface plots obtained for circularity error are found to be of almost similar trend to that obtained for cylindricity error. In addition, main effect of all the drilling parameters (highest impact with cutting speed and least

Fig. 8 3D surface plots for CE with: **a** CS and FR, **b** CS and PA, **c** FR and PA



contributions with the point angle) is seen identical for both circularity error and cylindricity error. Therefore, it is interesting to test the presence of relative dependency among the circularity error and cylindricity error.

3.2 Testing dependency among the circularity and cylindricity error

The dependency among the outputs is to be checked with large (say, 1000) database. It is impractical to conduct one thousand experiments for the said purpose. Therefore, one thousand datasets of drilling parameters (CS, FR, and PA) are randomly generated and predicted the circularity and cylindricity error from the derived regression equations (Eqs. 11–12). Best fit curve and correlation coefficient are the performance indicators, used to examine the relative dependency among the outputs. For the one thousand data points, the best fit curve for cylindricity error was found to have third-order nonlinear relation with circularity error (refer Fig. 9). It is observed that cylindricity error increases proportionally with circularity error and mathematical relationship among the outputs is expressed as shown in Eq. 13. The derived equation possesses good correlation coefficient value equal to 0.89. Therefore, cylindricity error is found to have strong dependent relationship with circularity error. Hence, cylindricity error can be predicted for the known values of circularity error through Eq. 13.

$$CE = -0.003568 + 0.1721 Ce - 0.2197 Ce^2 + 0.3643 Ce^3 \quad (13)$$

3.3 Testing of prediction accuracy

The nonlinear models developed for SR, TF, Ce, and CE showed good correlation coefficient with a value equal

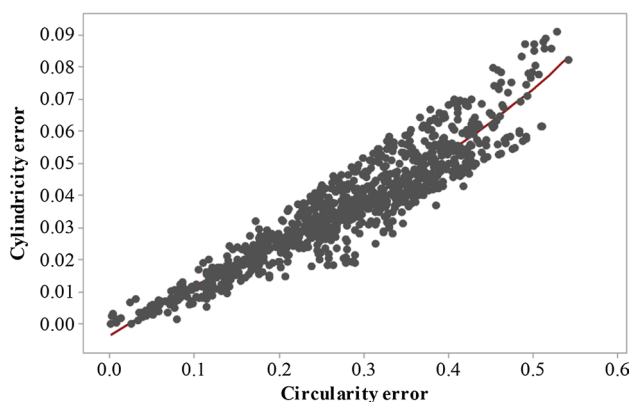


Fig. 9 Cylindricity error relationship with circularity error

to 0.9478, 0.9771, 0.9743, and 0.9839, respectively. The practical utility of these models is tested for ten random experimental cases which are presented in “Appendix 1.” The measured outputs for the experimental trials of random ten test cases are presented in “Appendix” 1. The model predicted and experimental output values are compared for all the ten experiments. The percent deviation in predicting ten experimental cases was found to lie both on the positive and negative sides with a range between -11.76 and $+10.48\%$ for SR, -9.24 and $+8.89\%$ for thrust force, -13.93 and $+14.71\%$ for circularity error, and -16.67 and $+14.29\%$ for cylindricity error, respectively (refer Tables 6 and 7). The average absolute percent deviation in prediction considering all ten experiments is found equal to 8.40% for SR, 5.41% for TF, 10.64% for Ce, and 10.35% for CE (refer Tables 6 and 7). The derived equations are useful for metal cutting industries that could predict the outputs for known set of input variables without the requirement of practical experiments.

3.4 Chip formation analysis

During drilling of aluminum alloy (Al 7075), the material plastically flows and is hard-pressed by the cutting tool, till the cutting forces (compressive) causes plastic deformation and in turn produces chips. In addition, the chips also undergo plastic deformations while ejecting upward through the flutes of twist drill and against the work piece. The chips are collected after drilling each hole under particular cutting conditions to perform chip morphology analysis (refer Fig. 10). Drilling quality characteristics (TF, SR, CE, and Ce) are directly related to the formed chips. Figure 10 shows the chips formed at different cutting speed (8, 14, 20 m/min) when the feed rate and point angle are maintained fixed at 0.18 mm/rev and 118° . The geometry of twist drill and cutting forces during drilling operation could raise the temperature at the cutting zone leads to formation of conical–helical chips. Increase in cutting speed, the length of the chip increases with simultaneous decrease in chip thickness. Similar observations are found in the literature [8]. Discontinuous chips are formed at low values of cutting speed (8 m/min). The discontinuous fan-shaped brake up and sequential short cone helical chips are converted to long helical chips, when the cutting speed raises from 8 to 14 m/min. The continuous long-ribbon-like chips ejected through the flute face of drill bit are observed at higher cutting speed of 20 m/min. Increase in feed rate tends to decrease the chip length with an increase in chip thickness (refer Fig. 10). The effect of feed rate on chip thickness is in good agreement with the published literature [2]. Long helical-shaped chips are transformed to short-type helical chips with an increase in

Table 6 Summary results of prediction accuracy of test cases: surface roughness and thrust force

Response	Surface roughness				Thrust force			
	Exp. SR, μm	CCD SR, μm	Percent deviation	Abs. percent deviation	Exp. TF, KN	CCD TF, KN	Percent deviation	Abs. percent deviation
1	1.02	1.14	-11.76	11.76	1.56	1.61	-3.21	3.21
2	1.35	1.27	5.93	05.93	1.76	1.66	5.68	5.68
3	2.64	2.82	-6.82	06.82	2.38	2.6	-9.24	9.24
4	1.17	1.28	-9.40	09.40	1.85	1.76	4.86	4.86
5	2.23	2.05	8.07	08.07	2.36	2.51	-6.36	6.36
6	1.35	1.49	-10.37	10.37	2.06	2.12	-2.91	2.91
7	1.25	1.37	-9.60	09.60	1.8	1.64	8.89	8.89
8	1.24	1.11	10.48	10.48	1.92	1.83	4.69	4.69
9	1.38	1.43	-3.62	03.62	1.54	1.59	-3.25	3.25
10	1.26	1.16	7.94	07.94	2.41	2.29	4.98	4.98
Minimum percent deviation: -11.76					-9.24			
Minimum percent deviation: +10.48					+8.89			
Average of absolute percent deviation:8.40					5.41			

Table 7 Summary results of prediction accuracy of test cases: circularity and cylindricity error

Output	Circularity error				Cylindricity error			
	Exp. Ce, mm	CCD Ce, mm	Percent Deviation	Abs. Percent Deviation	Exp. CE, mm	CCD CE, mm	Percent Deviation	Abs. Percent Deviation
1	0.438	0.499	-13.93	13.93	0.051	0.059	-15.69	15.69
2	0.278	0.251	9.71	9.71	0.014	0.012	14.29	14.29
3	0.514	0.546	-6.23	6.23	0.083	0.093	-12.05	12.05
4	0.452	0.42	7.08	7.08	0.060	0.059	1.67	1.67
5	0.373	0.404	-8.31	8.31	0.066	0.073	-10.61	10.61
6	0.250	0.277	-10.80	10.80	0.035	0.039	-11.43	11.43
7	0.189	0.214	-13.23	13.23	0.021	0.023	-9.52	9.52
8	0.034	0.029	14.71	14.71	0.011	0.01	9.09	9.09
9	0.160	0.181	-13.13	13.13	0.012	0.014	-16.67	16.67
10	0.248	0.225	9.27	9.27	0.040	0.039	2.50	2.50
Minimum percent deviation: -13.93					-16.67			
Minimum percent deviation: +14.71					+14.29			
Average of absolute percent deviation: 10.64					10.35			

chip thickness observed, when the feed rate was raised from 0.13 to 0.18 mm/rev. Loose fragmented chips are observed at higher feed rate of 0.25 mm/rev, due to excessive feeding. Increase in point angle showed increased arc length and radius of the chips. This occurs because the exposed large flank face produces continuous chips, as a result of interface friction at workpiece and cutting edge. The chip morphology (length, thickness, radius, and so on) changes with drilling parameters are due to change in cutting forces and working temperature.

3.5 Summary of results of CRITIC method

Determining single optimal parameter combination for multiple outputs (surface roughness, circularity error, cylindricity error, and thrust force) of drilling process is often difficult. This is because of the difference in significant and insignificant terms determined for the responses (refer Table 5). For example, feed rate is insignificant for circularity error, whereas significant for other outputs. All interaction terms ($A \times B$, $A \times C$, $B \times C$) are found significant for cylindricity error, whereas those terms were seen to

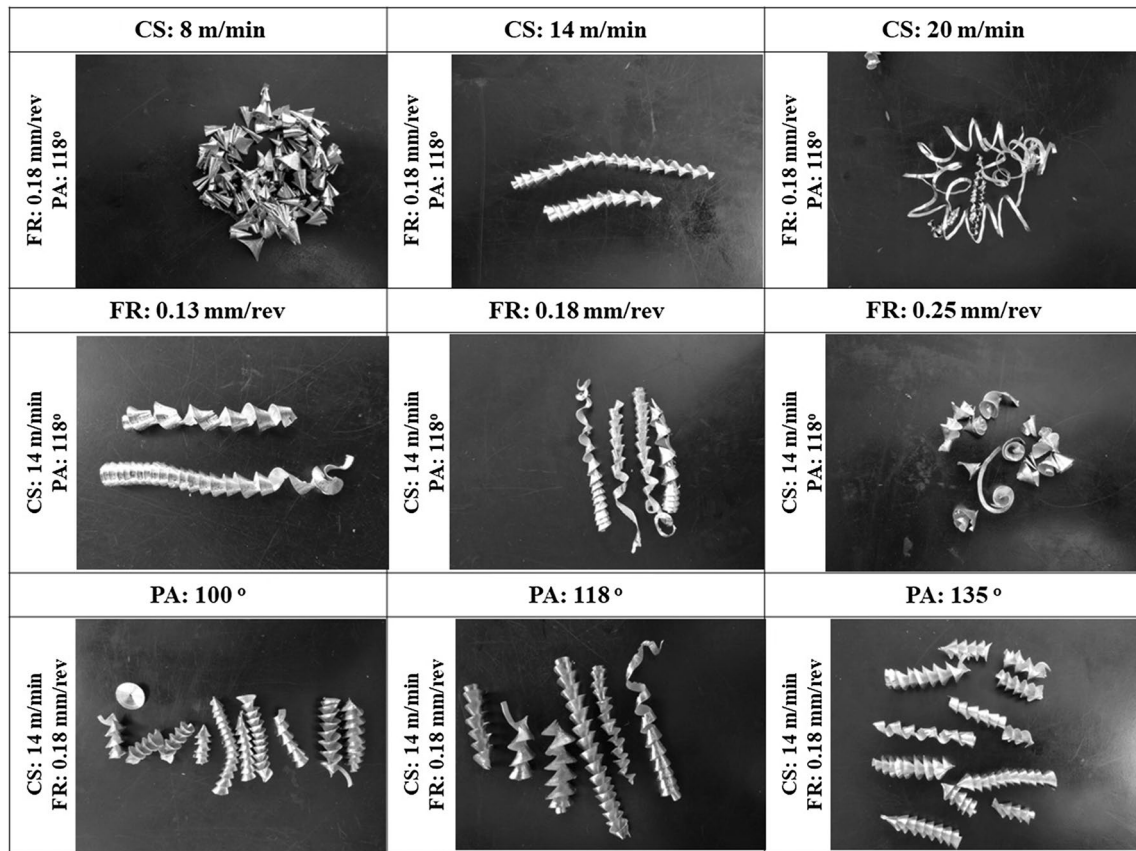


Fig. 10 Chip formation tested for different drilling conditions

be insignificant for thrust force and circularity error. Case studies involving assigning equal weights and maximum weight for individual output results in local solution (i.e., better solution for one output provided compromising solution with the rest). Therefore, determining weights based on experimental data could result in optimal condition for all outputs. CRITIC method is applied to determine the weights for an objective function, which do not require human intervention for a process that results in ease of decision making. CRITIC method is applied to determine the weights for all outputs (SR, Ce, CE, and TF). Face-centered central composite design (FCCD) based on sixteen experiments is treated as alternatives for decision-making process (refer Table 3). The output values of all 16 experimental trials are normalized between the ranges of 0 and 1 using Eq. 2. The results of normalized values are presented in Table 8. The standard deviation (SD) values corresponding to each output are determined using Eq. 3, and the corresponding values are presented in Table 8.

Table 9 presents the correlation coefficient of each criteria determined using Eq. 4. The obtained symmetry matrix ($m \times m$) value of Table 8 is subtracted with one, and the computed sum of all the responses is presented in Table 9.

Table 8 Normalized values of responses—CRITIC method

Exp. no	Responses			
	Ce	CE	TF	SR
1	0.928	0.841	0.942	1.000
2	0.223	0.561	1.000	0.978
3	1.000	1.000	0.486	0.830
4	0.280	0.573	0.400	0.558
5	0.790	0.988	0.806	0.915
6	0.161	0.207	0.007	0.625
7	0.937	1.000	0.581	0.915
8	0.688	0.768	0.430	0.723
9	0.666	0.756	0.473	0.652
10	0.289	0.707	0.435	0.545
11	0.169	0.439	0.750	0.821
12	0.740	0.976	0.854	0.665
13	0.646	0.866	0.343	0.598
14	0.197	0.476	0.694	0.558
15	0.000	0.000	0.000	0.000
16	0.718	0.756	0.264	0.884
SD	0.3288	0.2920	0.3001	0.2449

Interesting to note that the circularity error and cylindricity error are found to have good correlation coefficient compared to other output correlations (Tables 9 and 10).

The weights of individual response are computed based on the criterion information using Eqs. 5–6. The estimated criterion information and weights of individual outputs are presented in Table 11. The weights corresponding to Ce, CE, SR, and TF are found equal to 0.2802, 0.1991, 0.1914, and 0.3293, respectively.

3.6 Summary of results of multi-objective optimization by meta-heuristic algorithms

The nonlinear models developed for drilling performance quality characteristics are shown better coefficient of correlation with a value close to 1 (refer Table 5). Further, the model tested for prediction accuracy with ten random experimental cases showed an average absolute percent deviation in prediction equal to 8.40% for SR, 5.41% for TF, 10.64% for Ce, 10.35% for CE, respectively (refer Tables 6 and 7). Therefore, the derived response equation is statistically adequate and reliable to use as a fitness or objective function for determining optimal parameter set with the help of four algorithms (GA, PSO, TLBO, and JAYA). The optimal, minimum, and maximum values of different responses are searched by four algorithms within the regression equation (refer Eqs. 9–12) subjected to input variable constraints as shown below,

$$8 < \text{cutting speed} > 20;$$

$$0.13 < \text{feed rate} > 0.25;$$

$$100 < \text{point angle} > 135.$$

Table 11 shows the weights correspond to each output function used to calculate the D_o value. Note that, all four algorithms are tested for solution accuracy with determining overall desirability value D_o and computational efforts with the convergence plot and maximum number of function evaluation.

3.6.1 Comparison of meta-heuristic algorithm performances

The solution accuracy of algorithms is dependent on appropriate choice of algorithm-specific parameters (GA:

Table 10 Determining the summation of different responses

	Ce	CE	TF	SR	Summation
Ce	0.000	0.102	0.689	0.398	1.188
CE	0.102	0.000	0.499	0.350	0.951
TF	0.689	0.499	0.000	0.342	1.530
SR	0.398	0.350	0.342	0.000	1.090

probability of crossover and mutation; PSO: inertia weight) and common parameters (population size and iterations). The computation complexity, time, and solution accuracy are dependent on number of function evaluation (population size x number of generations) and D_o value in determining the optimal drilling conditions. Figure 11a–b shows the computed overall desirability value and maximum number of function evaluation correspond to each meta-heuristic algorithm. JAYA algorithm requires minimum number of function evaluation (population size x iterations: $30 \times 40 = 1200$) in order to determine the maximum fitness or overall desirability value (refer Fig. 11b). GA and PSO require maximum number of function evaluation with a value equal to 14,000 and 8000, respectively. GA and PSO require tuning of both algorithm-specific and common parameters, which increases both computation time and efforts. However, TLBO requires tuning of only common parameters but requires 2400 function evaluations to determine highest desirability value. The convergence plot of four algorithms (GA, PSO, TLBO, and JAYA) is tested against the fitness or overall desirability value is shown in Fig. 11c. It was observed that JAYA algorithm converges to 0.9679 for 40 iterations, TLBO algorithm converges to 0.9546 for 80 iterations, PSO algorithm converges to 0.951 for 100 iterations, and GA converges to 0.9426 for 140 iterations, respectively. JAYA algorithm produced better performances (highest global desirability value, minimum number of function evaluation, and iterations) might be due to their simplified approach in determining solutions and no tuning of algorithm-specific parameters. Although TLBO and JAYA algorithm performances are comparable, JAYA algorithm determined optimal drilling conditions are recommended both in terms of solution accuracy and simplicity in computation (refer Fig. 11a and Table 12).

Table 9 Correlation coefficient of responses

	Ce	CE	TF	SR
Ce	1.000	0.898	0.311	0.602
CE	0.898	1.000	0.501	0.650
TF	0.311	0.501	1.000	0.658
SR	0.602	0.650	0.658	1.000

Table 11 Determine the weights of different responses

Criteria	Cj	Wj
Circularity error	0.3907	0.2802
Cylindricity error	0.2776	0.1991
Thrust force	0.4591	0.3293
Surface roughness	0.2669	0.1914

Fig. 11 Performances of optimization algorithms with: **a** overall desirability value **b** maximum number of function evaluation, **c** fitness or Do vs. number of iterations

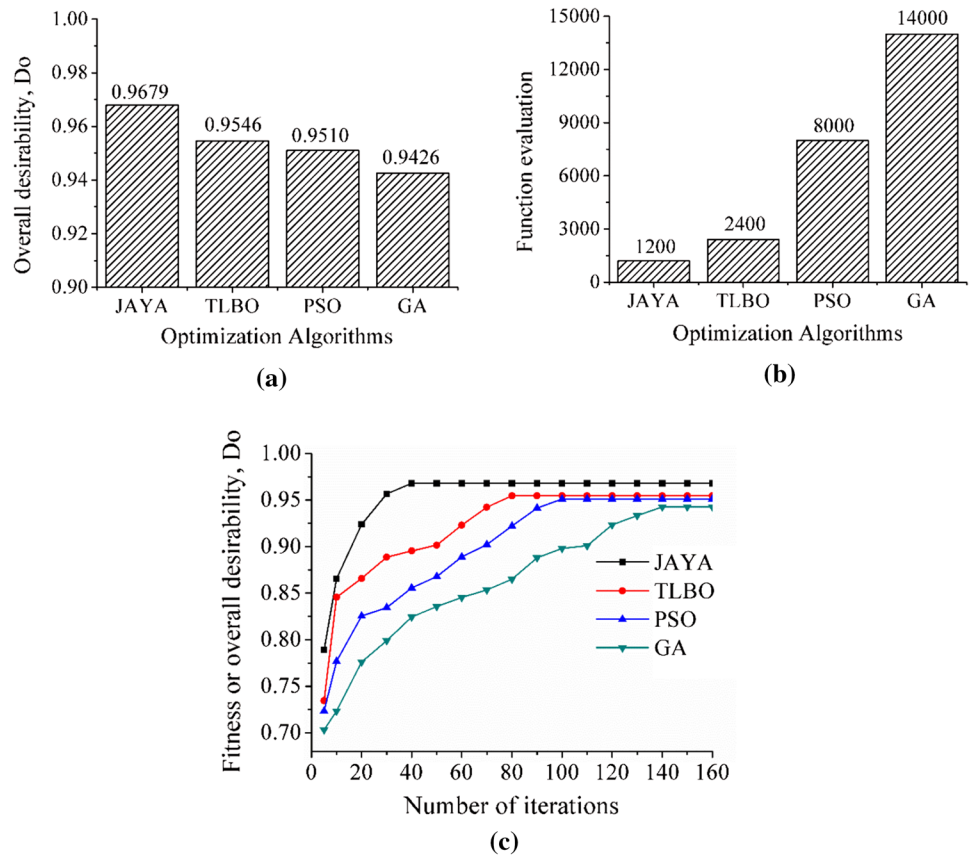


Table 12 Summary of results of optimized drilling conditions of different models

Model	Optimal model Parameters	Responses	Input variables
JAYA	Population size (10–160): 30 Maximum iterations (10–200): 40	Ce: 0.0373 mm CE: 0.01038 mm SR: 0.9864 μm TF: 1.482 KN	CS: 20 m/min FR: 0.1445 mm/rev PA: 100°
TLBO	Population size (10–160): 60 Maximum iterations (10–200): 80	Ce: 0.0365 mm CE: 0.00076 mm SR: 1.036 μm TF: 1.705 KN	CS: 17.07 m/min FR: 0.1807 mm/rev PA: 100°
PSO	Inertia weight (0–1): 0.8 Swarm size (50–160): 80 Maximum iterations (20–200): 100	Ce: 0.0635 mm CE: 0.0041 mm SR: 1.034 μm TF: 1.694 KN	CS: 16.41 m/min FR: 0.177 mm/rev PA: 100°
GA	Probability of crossover (0.5–1): 0.8 Probability of mutation (0.01–0.3): 0.1 Population size (40–160): 100 Maximum generations (20–250): 140	Ce: 0.148 mm CE: 0.022 mm SR: 0.938 μm TF: 1.543 KN	CS: 16.41 m/min FR: 0.177 mm/rev PA: 100°

3.7 Confirmation experiments

JAYA algorithm recommended optimal drilling conditions (CS: 20 m/min; FR: 0.15 mm/rev; and PA: 100°) are tested experimentally to validate the optimization technique corresponding to output performances. JAYA algorithm

recommended higher cutting speed with low values of feed rate, and point angle as optimal drilling conditions. Minimized friction coefficient on tool face, good rotational stability ensures the drill bit to pierce the work material without vibration at optimal drilling conditions causes reduced thrust force, circularity and cylindricity error and surface

roughness values [2, 8, 39, 59–61]. The resulted experimental output data are found equal to 0.0406 mm for circularity error, 0.0115 mm for cylindricity error, 0.92 μm for surface roughness, and 1.43 KN for thrust force, respectively. The comparison of predicted and experimental values resulted with a percent error of 10.8% for Ce, 8.9% for CE, 6.73% for SR, and 3.51% for TF. JAYA algorithm determined optimal drilling conditions can be used in industries to get better quality in drilled holes.

4 Conclusions

The present work focused on experimental modeling and optimization of drilling performance characteristics (circularity error, cylindricity error, thrust force, and surface roughness) by utilizing CCD-based experiments and advanced algorithm tools like (JAYA, PSO, TLBO, and GA), respectively. Based on the study, the following conclusions are drawn:

- All main effect factors (point angle, cutting speed, and feed rate) are found significant for all the quality characteristics, except feed rate for circularity error, but no influencing interaction among the factor is observed for thrust force and circularity error, while parameter, i.e., feed rate interaction with point angle, is significant for cylindricity error, but found insignificant for Ce, SR, and TF. Cutting speed has also showed highest contribution followed by point angle and feed rate toward Ce, CE, and SR. The feed rate has showed maximum impact on the thrust force.
- The developed nonlinear models for all responses produced better fit with a coefficient of correlation value close to 1. The average absolute percent deviation in prediction of responses of ten experimental cases was found equal to 8.40% for SR, 5.41% for TF, 10.64% for Ce, 10.35% for CE, respectively.
- The Ce showed third-order relationship with CE with a coefficient of correlation value equal to 0.89. The better correlation coefficient signifies that the unknown values of cylindricity error can be predicted approximately for the known values of circularity error with the derived mathematical expression.
- Chip morphology analysis showed increase in cutting speed (8–24 m/min) tends to increase the chip length with decrease in chip thickness. Chip length decreases with increase in chip thickness observed with increase in feed rate (0.13 to 0.25 mm/rev). Increase in point angle (100 to 135°) resulted in increased arc length and radius of the formed chips.
- CRITIC method estimated the weights associated with each quality characteristics (SR, TF, Ce, and CE) from experimental data. The weight fractions for SR, TF, Ce, and CE are found equal to 0.1914, 0.3293, 0.2802, and 0.1991, respectively.
- Four algorithms (JAYA, TLBO, PSO, and GA) are tested for their performances (solution accuracy and computation) in determining the optimal drilling parameter condition for multiple quality characteristics. JAYA algorithm outperformed other algorithms in determining highest overall desirability value at reduced number of function evaluation. Although TLBO algorithm results are comparable with JAYA, their two phases (teacher and learner) working method increases the computation efforts and time.
- JAYA algorithm determined optimal drilling conditions resulted experimentally with better drilled hole quality at reduced thrust force.

Appendix 1

See Table 13.

Table 13 Input–output data of test cases

Test cases	Cutting variables			Machining quality characteristics			
	CS, m/min	FR, mm/rev	PA, °	SR, μm	Ce, mm	CE, mm	TF, KN
1	8	0.13	110	1.02	0.438	0.051	1.56
2	8	0.18	100	1.35	0.278	0.014	1.76
3	8	0.25	130	2.64	0.514	0.083	2.38
4	14	0.13	118	1.17	0.452	0.060	1.85
5	14	0.25	135	2.23	0.373	0.066	2.36
6	14	0.25	100	1.35	0.250	0.035	2.06
7	20	0.13	130	1.25	0.189	0.021	1.80
8	20	0.18	110	1.24	0.034	0.011	1.92
9	20	0.13	135	1.38	0.160	0.012	1.54
10	20	0.25	118	1.26	0.248	0.040	2.41

Declarations

Conflict of interest Authors declare that there is no potential conflict of interest in publishing this article.

References

- Giasin K, Hodzic A, Phadnis V, Ayvar-Soberanis S (2016) Assessment of cutting forces and hole quality in drilling Al2024 aluminium alloy: experimental and finite element study. *Int J Adv Manuf Tech* 87(5–8):2041–2061
- Farid AA, Sharif S, Idris MH (2011) Chip morphology study in high speed drilling of Al–Si alloy. *Int J Adv Manuf Tech* 57(5–8):555–564
- Astakhov VP (2011) Drilling. In *Modern Machining Technology*. Woodhead Publishing, pp. 79–212
- Koklu U (2012) Influence of process parameters and the mechanical properties of aluminium alloys on the burr height and the surface roughness in dry drilling. *Mate & Tech* 46(2):103–108
- Mohamed E, Houcine M, Boukhoulda FB (2013) Effect of drilling parameters on hole quality. *Int J Mining, Meta & Mech Eng* 1(4):254–257
- Abidin NWZ, Ab Rashid MFF, Mohamed NMZN (2019) A review of multi-holes drilling path optimization using soft computing approaches. *Arch Compu Methd in Engg* 26(1):107–118
- Rivero A, Aramendi G, Herranz S, de Lacalle LL (2006) An experimental investigation of the effect of coatings and cutting parameters on the dry drilling performance of aluminium alloys. *Int J Adv Manuf Tech* 28(1–2):1–11
- Samy GS, Kumaran ST (2017) Measurement and analysis of temperature, thrust force and surface roughness in drilling of AA (6351)-B4C composite. *Measur* 103:1–9
- Kurt M, Kaynak Y, Bagci E (2008) Evaluation of drilled hole quality in Al 2024 alloy. *Int J Adv Manuf Tech* 37(11–12):1051–1060
- Pramanik A, Basak AK, Uddin MS, Shankar S, Debnath S, Islam MN (2019) Burr formation during drilling of mild steel at different machining conditions. *Mater and Manuf Proce* 34(7):726–735
- Rahim EA, Sasahara H (2011) A study of the effect of palm oil as MQL lubricant on high speed drilling of titanium alloys. *Tribo Int* 44(3):309–317
- Bagci E, Ozcelik B (2006) Analysis of temperature changes on the twist drill under different drilling conditions based on Taguchi method during dry drilling of Al 7075–T651. *Int J Adv Manuf Tech* 29(7–8):629–636
- Nouari M, List G, Girof F, Coupard D (2003) Experimental analysis and optimisation of tool wear in dry machining of aluminium alloys. *Wear* 255(7–12):1359–1368
- Davim JP (2011) *Modern machining technology: a practical guide*. Elsevier
- Gaitonde V, Karnik SR, Rubio JC, Correia AE, Abrao AM, Davim JP (2008) Analysis of parametric influence on delamination in high-speed drilling of carbon fiber reinforced plastic composites. *J Mater Process Technol* 203(1–3):431–438
- Ueda T, Nozaki R, Hosokawa A (2007) Temperature measurement of cutting edge in drilling-effect of oil mist. *CIRP Ann* 56(1):93–96
- Matsumura T, Hori I, Shirakashi T (2010) Analysis of cutting temperature in drilling process. *Int J Mater Formg* 3(1):499–502
- Davoudinejad A, Ashrafi SA, Hamzah RIR, Niazi A (2012) Experimental analysis of wear mechanism and tool life in dry drilling of Al2024. *Adv Mater Resea* 566:217–221
- Rahim EA, Kamdani K, Sharif S (2008) Performance evaluation of uncoated carbide tool in high speed drilling of Ti6Al4V. *J Adv Mech Design Sys and Manuf* 2(4):522–531
- Prasanna J, Karunamoorthy L, Raman MV, Prashanth S, Chordia DR (2014) Optimization of process parameters of small hole dry drilling in Ti–6Al–4V using Taguchi and grey relational analysis. *Measur* 48:346–354
- Liao YS, Chen YC, Lin HM (2007) Feasibility study of the ultrasonic vibration assisted drilling of Inconel superalloy. *Int J Machine Tools and Manuf* 47(12–13):1988–1996
- Batzer SA, Haan DM, Rao PD, Olson WW, Sutherland JW (1998) Chip morphology and hole surface texture in the drilling of cast aluminum alloys. *J Mater Proces Techn* 79(1–3):72–78
- Knight SP, Pohl K, Holroyd NJH, Birbilis N, Rometsch PA, Muddle BC, Goswami R, Lynch SP (2015) Some effects of alloy composition on stress corrosion cracking in Al–Zn–Mg–Cu alloys. *Corro Sci* 98:50–62
- Ghasemi AH, Khorasani AM, Gibson I (2018) Investigation on the effect of a pre-center drill hole and tool material on thrust force, surface roughness, and cylindricity in the drilling of Al7075. *Mater* 11(1):140
- Çakıroğlu R, Acır A (2013) Optimization of cutting parameters on drill bit temperature in drilling by Taguchi method. *Measur* 46(9):3525–3531
- Kilickap E (2010) Modeling and optimization of burr height in drilling of Al-7075 using Taguchi method and response surface methodology. *Int J Adv Manuf Tech* 49(9–12):911–923
- Kao JY, Hsu CY, Tsao CC (2019) Experimental study of inverted drilling Al-7075 alloy. *Int J Adv Manuf Tech* 102(9–12):3519–3529
- Ucun İ (2016) 3D finite element modelling of drilling process of Al7075-T6 alloy and experimental validation. *J Mech Sci and Tech* 30(4):1843–1850
- Çiçek A, Kıvık T, Ekici E (2015) Optimization of drilling parameters using Taguchi technique and response surface methodology (RSM) in drilling of AISI 304 steel with cryogenically treated HSS drills. *J Intell Manuf* 26(2):295–305
- Kilickap E, Huseyinoglu M, Yardimeden A (2011) Optimization of drilling parameters on surface roughness in drilling of AISI 1045 using response surface methodology and genetic algorithm. *Int J Adv Manuf Tech* 11(8):79–88
- Lim WCE, Kanagaraj G, Ponnambalam SG (2016) A hybrid cuckoo search-genetic algorithm for hole-making sequence optimization. *J Intell Manuf* 27(2):417–429
- Yang HC, Liu KJ, Hung MH (2012) Drill-path optimization with time limit and thermal protection. *Adv Mat Res* 579:153–159
- Shahrajabian H, Farahnakian M (2013) Modeling and multi-constrained optimization in drilling process of carbon fiber reinforced epoxy composite. *Int J Precis Eng Man* 14(10):1829–1837
- Gaitonde VN, Karnik SR (2012) Minimizing burr size in drilling using artificial neural network (ANN)-particle swarm optimization (PSO) approach. *J Intell Manuf* 23(5):1783–1793
- Patel P, Nakum B, Abhishek K, Kumar VR (2018) Machining performance optimization during plasma arc cutting of AISI D2 steel: application of FIS, nonlinear regression and JAYA optimization algorithm. *J Braz Soc of Mech Sci Eng* 40(4):240
- Alinezhad A, Khalili J (2019) CRITIC Method. In: *New Methods and Applications in Multiple Attribute Decision Making (MADM)* (pp. 199–203). Springer, Cham.
- Žižović M, Miljković B, Marinković D (2020) Objective methods for determining criteria weight coefficients: a modification of the CRITIC method. *Decis Making Appl Manage Eng* 3(2):149–161
- Zhang JZ, Chen JC (2009) Surface roughness optimization in a drilling operation using the Taguchi design method. *Mater Manuf Proces* 24:459–467

39. Díaz-Álvarez A, Díaz-Álvarez J, Santiuste C, Miguélez MH (2019) Experimental and numerical analysis of the influence of drill point angle when drilling biocomposites. *Compos Struct* 209:700–709
40. Patel GM, Lokare D, Chate GR, Parappagoudar MB, Nikhil R, Gupta K (2020) Analysis and optimization of surface quality while machining high strength aluminium alloy. *Measure* 152:107337
41. Madić M, Radovanović M (2015) Ranking of some most commonly used nontraditional machining processes using ROV and CRITIC methods. *UPB Sci Bull Ser D* 77(2):193–204
42. Tuş A, Adal EA (2019) The new combination with CRITIC and WASPAS methods for the time and attendance software selection problem. *Opsear* 56(2):528–538
43. Ting TO, Lee TS (2012) Drilling optimization via particle swarm optimization. *Int J Swarm Intell Res* 3(1):43–54. <https://doi.org/10.4018/jsir.2012010103>
44. Mirjalili S (2015) The ant lion optimizer. *Adv Eng Softw* 83:80–98. <https://doi.org/10.1016/j.advengsoft.2015.01.010>
45. Mirjalili S, Mirjalili SM, Lewis A (2014) Grey wolf optimizer. *Adv Eng Softw* 69:46–61. <https://doi.org/10.1016/j.advengsoft.2013.12.007>
46. Gandomi AH, Yang X, Alavi AH (2013) Cuckoo search algorithm: A metaheuristic approach to solve structural optimization problems. *Engg with Compu* 29:17–35. <https://doi.org/10.1007/s00366-011-0241-y>
47. Rao RV, Kalyankar VD (2013) Parameter optimization of modern machining processes using teaching–learning-based optimization algorithm. *Eng Appl Artif Intell* 26(1):524–531
48. Rao RV (2016) Jaya: a simple and new optimization algorithm for solving constrained and unconstrained optimization problems. *Int J of Ind Eng Comp* 7(1):19–34
49. Rao RV (2019) *Jaya: an advanced optimization algorithm and its engineering applications*. Springer International Publishing, Switzerland
50. Rao RV (2020) Rao algorithms: three metaphor-less simple algorithms for solving optimization problems. *Int J Ind Engg Compu* 11:107–130. <https://doi.org/10.5267/j.ijiec.2019.6.002>
51. Rao RV, Savsani VJ, Vakharia DP (2011) Teaching-learning-based optimization: a novel method for constrained mechanical design optimization problems. *Comput Aided Des* 43(3):303–315. <https://doi.org/10.1016/j.cad.2010.12.015>
52. Rao RV, Savsani VJ, Balic J (2012) Teaching–learning-based optimization algorithm for unconstrained and constrained real-parameter optimization problems. *Eng Opt* 44(12):1447–1462
53. Venkata RR, Dhiraj PR, Balic J (2017) Multi-objective optimization of abrasive waterjet machining process using Jaya algorithm and PROMETHEE Method. *J Intel Manuf* 30(5):2101–2127
54. Venkata RR, Dhiraj PR, Balic J (2017) A multi-objective algorithm for optimization of modern machining processes. *Engg Appl of Artif Intel* 61:103–125
55. Sivanandam SN, Deepa SN (2008) *Genetic algorithms*. In *Introduction to genetic algorithms*. Springer, Berlin, pp. 15–37.
56. Karaboga D, Basturk B (2007) A powerful and efficient algorithm for numerical function optimization: artificial bee colony (ABC) algorithm. *J global opti* 39(3):459–471
57. Ding Y, Zhang W, Yu L, Lu K (2019) The accuracy and efficiency of GA and PSO optimization schemes on estimating reaction kinetic parameters of biomass pyrolysis. *Energy* 176:582–588
58. Sierra MR, Coello CAC (2005) Improving PSO-based multi-objective optimization using crowding, mutation and ϵ -dominance. *Evolu Multi-Criterion Opti*, pp. 505–19.
59. Heisel U, Pfeifroth T (2012) Influence of point angle on drill hole quality and machining forces when drilling CFRP. *Proc Cirp* 1:471–476
60. Krishnaraj V, Prabukarthi A, Ramanathan A, Elanghovan N, Kumar MS, Zitoune R, Davim JP (2012) Optimization of machining parameters at high speed drilling of carbon fiber reinforced plastic (CFRP) laminates. *Compos B Eng* 43(4):1791–1799
61. Sultan AZ, Sharif S, Kurniawan D (2015) Effect of machining parameters on tool wear and hole quality of AISI 316L stainless steel in conventional drilling. *Procedia Manuf* 2:202–207

Publisher's Note Springer Nature remains neutral with regard to jurisdictional claims in published maps and institutional affiliations.